

Preparation of Artificial Skin that Mimics Human Skin Surface and Mechanical Properties

Rana Shimizu and Yoshimune Nonomura*

Department of Biochemical Engineering, Graduate School of Science and Engineering, Yamagata University, 4-3-16 Jonan, Yonezawa 992-8510, JAPAN

Abstract: We have developed an artificial skin that mimics the morphological and mechanical properties of human skin. The artificial skin comprises a polyurethane block possessing a microscopically rough surface. We evaluated the tactile sensations when skin-care cream was applied to the artificial skin. Many subjects perceived smooth, moist, and soft feels during the application process. Cluster analysis showed that these characteristic tactile feels are similar to those when skin-care cream is applied to real human skin. Contact angle analysis showed that an oil droplet spread smoothly on the artificial skin surface, which occurred because there were many grooves several hundred micrometers in width on the skin surface. In addition, when the skin-care cream was applied, the change in frictional force during the dynamic friction process increased. These wetting and frictional properties are important factors controlling the similarity of artificial skin to real human skin.

Key words: artificial skin, texture, polyurethane, rough surface

1 INTRODUCTION

Artificial skin has been used in various fields. For example, engraftment ability is essential if the artificial skin is used as a substitute for trauma to therapy¹⁻³⁾. On the other hand, it is desirable that surface properties and tactile texture of humanoid robots and tactile sensors are similar with those of real human skin. Then, some artificial skins which imitate the morphology, hardness and physical properties of human skin have been developed to realize human skin-like tactile texture⁴⁻⁹⁾.

For evaluating the tactile texture in application process of liquid cosmetics such as a skin cream, lotion and liquid foundation, the evaluation conditions should be mimicked with those when the liquid material is spread on the skin surface^{10,11)}. Dussaud *et al.* showed that penetration on the skin surface is caused by the spreading of liquid material through microscopic grooves on the skin surface¹²⁾. This finding predicts that not only the elastic structure but also the mesh-like rough structure is an important factor to mimic the application process of liquid cosmetics on skin surface.

In this study, we developed an artificial skin model that mimics the wetting characteristics of human skin for accurate evaluation of the tactile texture of the liquid cosmetics. Thin polyurethane film was used for the model surface

because the surface energy of keratin, which is the main component of the horny layer of human skin, is close to that of the polymer material^{13,14)}. This model surface was fixed on a soft polyurethane substrate to obtain an artificial skin model. We evaluated the effect of surface structure and hardness on the tactile texture. Finally, the physical properties including surface shape, wettability and frictional property were evaluated to show the relationship between tactile texture and physical properties of artificial skin.

2 EXPERIMENTAL PROCEDURES

2.1 Materials and preparation of artificial skin models

We prepared artificial skin models comprising a hard surface film and a soft substrate (Fig. 1(a)). The surface films **a** and **b** and the substrates **1-3** were as follows: a polyurethane film **a** (thickness 0.012 mm, *Sara-ri*, Shemoa Co., Ltd, Osaka, Japan), a polyurethane film **b** (thickness 0.005 mm, *Sara-ri air*, Shemoa Co., Ltd, Osaka, Japan), a polyurethane substrate **1** (ASKER C hardness 0), a polyurethane substrate **2** (ASKER C 5), and a polyurethane substrate **3** (ASKER C 15). Asker C hardness, which is a standard of the Society of Rubber Science and Technology,

*Correspondence to: Yoshimune Nonomura, Department of Biochemical Engineering, Graduate School of Science and Engineering, Yamagata University, 4-3-16 Jonan, Yonezawa 992-8510, JAPAN

E-mail: nonoy@yz.yamagata-u.ac.jp

Accepted August 18, 2017 (received for review July 4, 2017)

Journal of Oleo Science ISSN 1345-8957 print / ISSN 1347-3352 online

<http://www.jstage.jst.go.jp/browse/jos/> <http://mc.manuscriptcentral.com/jjocs>

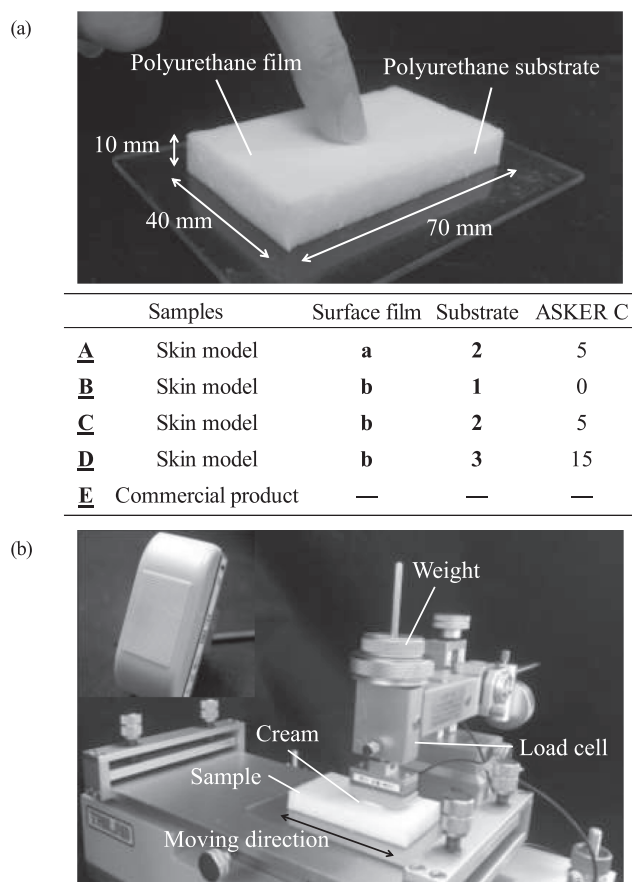


Fig. 1 Images depicting the artificial skin model (a) and the friction evaluation system with a human finger model (b).

Japan, is evaluated by shore round style durometers. To obtain the polyurethane substrates, a mixture of 90 g of a main component (polyol-based, Exseal Co., Ltd, Gifu, Japan) and 30 g of a curing agent (isocyanate-based, Exseal Co., Ltd, Gifu, Japan) was poured into an acrylic resin mold (size = 40 × 70 × 10 mm) covered with a fluororesin sheet (Naflon PTFE, 0.05 mm thick, Nichias Co., Ltd, Tokyo, Japan) and left at room temperature for approximately 24 hours. To prepare artificial skin models **A** to **D** having different surface thicknesses and substrate hardness, either film **a** or **b** was attached to one of the substrates. Since acrylic adhesive is coated on one side of films **a** and **b**, it is possible to fix the film on urethane substrate. Figure 1(a) shows the combination of the film and substrate lead to models **A–D**. In addition, a commercially available product (“bio skin plate,” polyurethane, thickness 5 mm, hardness (JIS A) 10, Beulax Co., Ltd, Saitama, Japan) was used for comparison (model **E**).

For tactile evaluation, two commercial skin-care creams were applied to the skin and skin models. The creams were water-in-oil (W/O) emulsion in which water droplets were dispersed in an oil phase and oil-in-water (O/W) emulsion in

which oil droplets were dispersed in water phase. The components of the W/O cream were as follows: water, mineral oil, petrolatum, glycerin, hydrogenatedpolyisobutene, cyclomethicone, microcrystalline wax, lanolin alcohol, paraffin, squalane, jojoba oil, decyloleate, octyldodecanol, aluminum distearate, magnesium stearate, magnesium sulfate, citric acid, sodium benzoate, and fragrance. The components of the O/W cream were as follows: water, glycerin, BG, isohexadecane, cetyl ethylhexanoate, ethanol, DPG, PEG-20, dimethicone, PEG-0.99, cetyl PEG / PPG-10/1 dimethicone, diphenyl siloxy phenyltrimethicone methicone, Tripoli hydroxystearic acid dipentaerythritol Riiru, sodium chloride, (behenate / eicosadiolate) glyceryl, arginine HCl, ubiquinone, thiocetic acid, soluble collagen, crucian bud extract, glucosyl hesperidin, mortierella oil, hydrolyzed elastin, yokuininekisu, clara extract, valerian rhizomes/root extract, vaseline triisostearate, zinc oxide, EDTA-3 sodium, cellulose gum, sodium citrate, agar, PEG-10 dimethicone, dextrin palmitate, citric acid, tocopherol, tetrahydrotetramethylcyclotetrasiloxane, tetradecene, phenoxyethanol, fragrance, iron oxide.

2.2 Tactile evaluation of artificial skin model

We evaluated the tactile texture using the visual analog scale method when the skin-care cream was applied to artificial skin models **A–E**. The tactile evaluation was performed under two conditions. In the first condition, 0.03 g of skin-care cream was applied on the artificial skin model by an index finger of the dominant hand. In the second condition, the skin-care cream was applied on the skin surface of the forearm of subjects. The application time of the skin-care cream on the skin model or human skin was 15 seconds, while the coating area was about $2.8 \times 10^3 \text{ mm}^2$ in either condition. The subjects were 20 women aged 20 to 25 years old. The feels used in the tactile evaluation were soft, hard, dry, moist, slippery, sticky, smooth, rough, cold, and hot, and each feel was scored in the range 0–10. These tactile evaluations were performed at a room temperature of $25 \pm 1^\circ\text{C}$ and a relative humidity of $50 \pm 5\%$. To categorize the skin models and real human skin based on their tactile texture scores, a hierarchical cluster analysis was performed (SPSS, IBM Co., Ward method). These tactile sensations were evaluated with two kinds of skin-care creams. All evaluations were conducted according to the principles expressed in the Declaration of Helsinki. The responsible party at Yamagata University confirmed that the ethics and safety of the present tests were acceptable.

2.3 Physical evaluation

The surface roughness of artificial skin models **A–E** was measured using a laser microscope LEXT OLS 4000 (Olympus, Osaka, Japan). The arithmetic mean roughness R_a was measured in three places at a measurement magnification of 20 times. The contact angles of 1.0 μL water

droplets and liquid paraffin droplets (Kanto Chemical Co., Tokyo, Japan) on the model surfaces were estimated by a sessile drop measuring method using a DM-501 contact angle meter obtained from Kyowa Interface Science (Saitama, Japan). Liquid droplets were dropped from the tip of a 22G tetrafluoroethylene-coated syringe (internal diameter: 0.4 mm, external diameter: 0.7 mm) using an automatic dispenser designed for the DM-501 instrument. The evaluation conditions were as follows: measurement interval = 150 ms, continuous measurement number = 2001, and measurement time = 5 min. All contact angles were measured at 10 different points.

The friction measurements were performed using a Tribo Master TL201Ts friction evaluation meter (Trinity Lab Inc., Tokyo, Japan), as shown in Fig. 1 (b). The specifications of the apparatus were as follows: measurement range = 0.098–19.6 N, vertical force = 0.098–4.9 N, sliding speed = 0.1–100 mm s⁻¹, and sliding distance = 1–100 mm; the apparatus possessed an AC servomotor. The frictional force was measured by fixing each model on a pedestal with double-sided tape (Nichiban Co., Tokyo, Japan) and rubbing

it with a contact probe loaded with 0.03 g of skin-care cream. The contact probe reflected the geometry and mechanical properties of real human fingers, and the probe surface contained 29 grooves (depth: 0.15 mm) carved at 0.5 mm intervals¹⁰. The friction conditions were as follows: sliding width = 50 mm, sliding speed = 100 mm s⁻¹, number of reciprocations = 12 reciprocations, load = 150 g, and sampling speed = 1 ms. These physical evaluations were performed at a temperature of 25 ± 1°C and a relative humidity of 50 ± 5%.

3 RESULTS

3.1 Tactile texture of artificial skin model

Figure 2(a) shows the tactile scores when the W/O skin-care cream was applied to each artificial skin model. Based on the ten tactile scores, artificial skin models and human skin were categorized into three groups. The characteristic feels of group I comprising human skin and model **B** were smooth, moist, and soft; the smooth feel scores of human

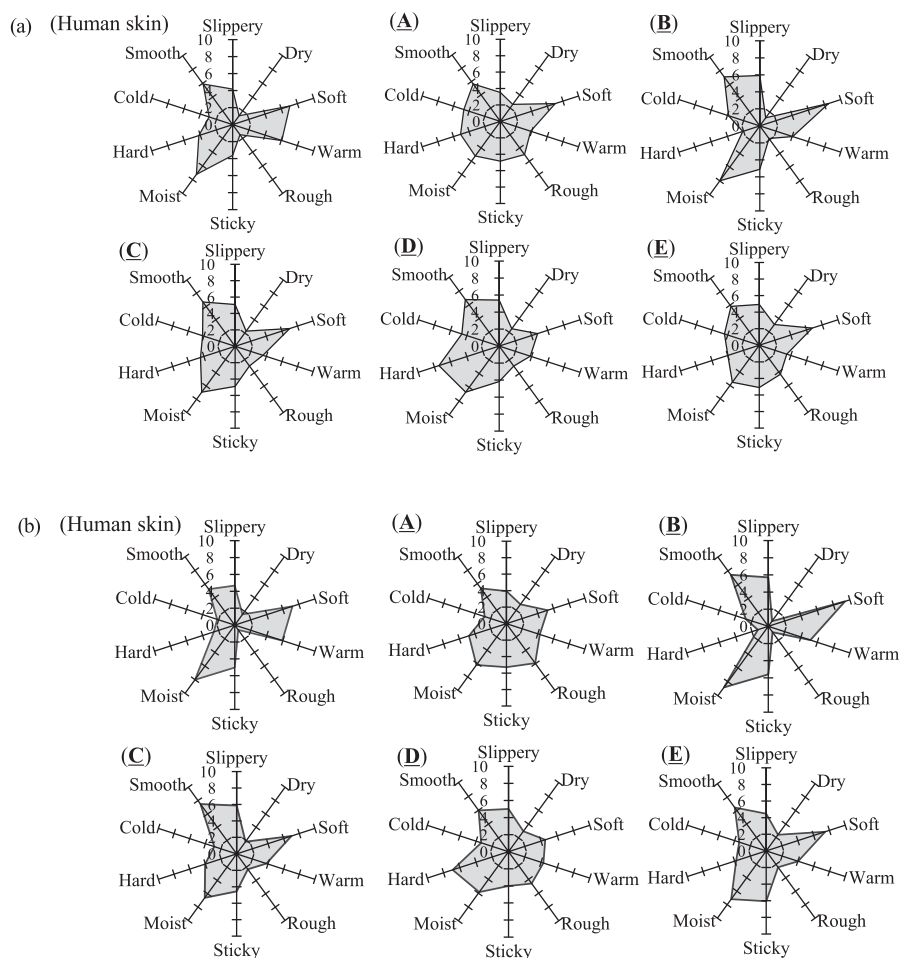


Fig. 2 Tactile textures of human skin and artificial skin models during the application of the W/O skin-care cream (a) and the O/W skin-care cream (b).

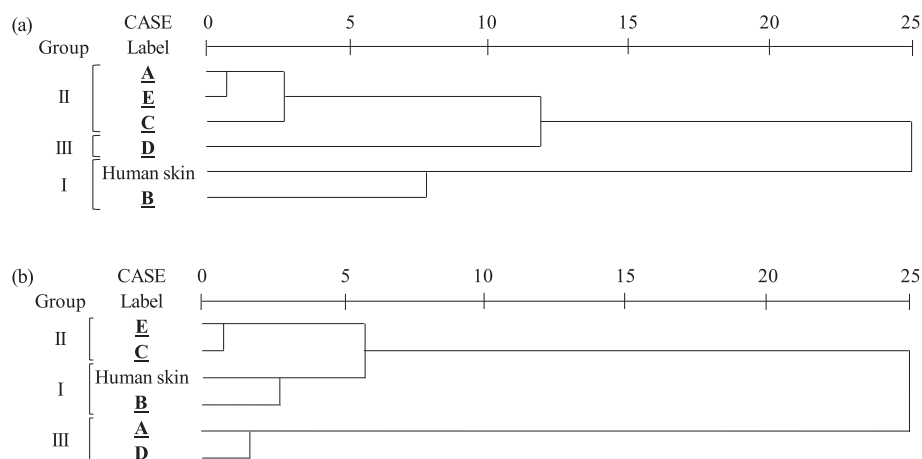


Fig. 3 Dendrogram of the textures of human skin and artificial skin models during the application of the W/O skin-care cream (a) and the O/W skin-care cream (b).

skin and model **B** were 5.9 ± 3.1 (average \pm standard deviation) and 7.1 ± 2.5 , the moist feel scores were 7.2 ± 2.2 and 8.0 ± 2.2 , and the soft feel scores were 7.1 ± 2.3 and 8.5 ± 1.3 , respectively. The feel of group II comprising models **A**, **C**, and **E** was soft, and the scores were 7.0 ± 2.2 , 7.0 ± 2.1 , and 6.7 ± 2.7 , respectively. In the case of group III comprising only model **D**, the characteristic feel was hard, and the score was 7.4 ± 2.1 . To confirm the suitability of the categorization, a hierarchical cluster analysis was performed using the tactile scores. **Figure 3(a)** shows the corresponding dendrogram, which contains three clusters that are similar to the above descriptions.

Figure 2(b) shows the tactile scores when the O/W skin-care cream was applied to each artificial skin model. Based on the tactile score, the artificial skin model and the human skin were classified into three groups as well as when the W/O skin-care cream was applied. The characteristic feels of group I comprising human skin and model **B** were smooth, moist, and soft; the smooth feel scores of human skin and model **B** were 5.3 ± 2.6 and 7.4 ± 2.1 , the moist feel scores were 8.0 ± 1.5 and 8.8 ± 1.0 , and the soft feel scores were 7.2 ± 1.8 and 9.4 ± 0.8 , respectively. The feel of group II comprising models **C** and **E** were soft, and the scores were 7.0 ± 2.0 and 7.5 ± 2.3 , respectively. In the case of group III comprising model **A** and **D**, the characteristic feel was hard, and the score were 4.8 ± 3.1 and 6.9 ± 2.2 , respectively. To confirm the suitability of the categorization, a hierarchical cluster analysis was performed using the tactile scores. **Figure 3(b)** shows the corresponding dendrogram, which contains three clusters that are similar to the above descriptions.

3.2 Shape and physical properties of artificial skin model

To determine the physical origin of the tactile textures of the artificial skin models, their surface shape, wettability, mechanical properties, and frictional properties were eval-

uated. First, the surface shape of each artificial skin model was evaluated. **Table 1** shows laser microscope images and R_a values of each model at a measurement magnification of 20 times. On each model, a rough structure was observed on the surface, ranging in size from tens to hundreds of micrometers. In the cases of model **A-D**, many grooves were formed when the backing sheet of the film **a** or **b** was removed after bonding the film to substrate **1-3**. At the present time, the mechanism of groove formation is unknown. The grooves may be created due to the reduced tension on the film when removing the backing sheet from the film **a** or **b**.

In particular, many grooves having widths of several hundred micrometers exist on artificial skin models **B**, **C**, and **D**, whose surfaces were covered with film **b**. The R_a values were 15.5 ± 2.2 , 12.3 ± 7.2 , and $8.3 \pm 0.3 \mu\text{m}$ for **B**, **C**, and **D**, respectively, even though the substrates were covered with the same film **b**. The surface roughness increased as the substrate became softer. In a layered structure comprising a hard thin film and a soft substrate, the surface layer can be strained by compressive stress. Ohzono *et al.* reported that fine wrinkles called “microwrinkles” were formed on such films¹⁵⁾. The wavelength of the wrinkles λ is described by

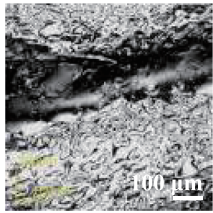
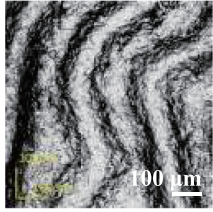
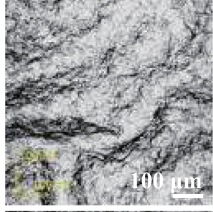
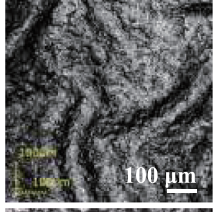
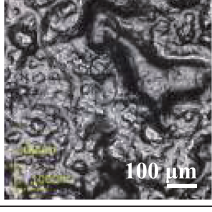
$$\lambda \propto h \left(\frac{E_f}{E_s} \right)^{\frac{1}{3}} (E_f > E_s) \quad (1)$$

where h is the thickness of the surface film, and E_f and E_s are the Young's moduli of the surface film and the soft substrate, respectively. The depth of the wrinkles A is given by

$$A \sim \lambda \left(\frac{\Delta}{w} \right)^{\frac{1}{2}} \quad (2)$$

where Δ/w is an imposed compressive strain¹⁶⁾. Equations (1) and (2) suggest that the wavelength and depth of the wrinkles depend on the ratio of the Young's modulus of the surface film to that of the soft substrate; the width and depth increase as the ratio E_f/E_s increases. This trend is

Table 1 Microscopic images and surface shape of each sample.

| Sample | Microscopic image | Surface shape | Contact angle / deg. | |
|-----------------|---|------------------------------------|----------------------|-----------------|
| | | $\times 20$ $R_a / \mu\text{m}$ | Water | Liquid paraffin |
| <u>A</u> |  | 13.0 ± 14.3 | 34.9 ± 4.7 | 21.5 ± 3.5 |
| <u>B</u> |  | 15.5 ± 2.2 | 40.8 ± 4.0 | 5.0 ± 4.1 |
| <u>C</u> |  | 12.3 ± 7.2 | 46.3 ± 6.0 | 8.5 ± 6.0 |
| <u>D</u> |  | 8.3 ± 0.3 | 42.0 ± 5.1 | 16.2 ± 2.6 |
| <u>E</u> |  | 7.6 ± 1.9 | 41.9 ± 5.6 | 23.2 ± 6.2 |

consistent with the present results. Comparing the models **B**, **C**, and **D**, whose surfaces are all covered with **b**, the surface roughness R_a of **B** is the largest because the substrate is the softest.

The wettability of the artificial skin toward the cream is also an important factor that dominates the tactile texture. The contact angles of water and liquid paraffin droplets are given in **Table 1**. Although the contact angle of water droplets was approximately 40° on all models, significant differences were observed for liquid paraffin droplets. The contact angles on models **B** and **E** were $5.0 \pm 4.1^\circ$ and $23.2 \pm 6.2^\circ$, which are the lowest and highest observed for all models. Although the surface of the models is covered with film **b** for **B**, **C**, and **D**, their contact angles are clearly different: $5.0 \pm 4.1^\circ$, $8.5 \pm 6.0^\circ$, and $16.2 \pm 2.6^\circ$, respectively.

Such differences in wettability are caused by the surface structure of the skin models. As mentioned in the last paragraph, the laser microscopic images of models **B**, **C**, and **D** show that the surface roughness increased as the substrate becomes softer. According to the Wenzel model, the roughness of solid surfaces enhances their hydrophilic/lipophilic properties¹⁷⁾. On model **B**, which has deep microwrinkles, the oil droplet forms a spherical lens with a low contact angle due to the large surface area¹⁸⁾. Another interesting phenomenon was the appearance of a wicking front. **Figure 4** shows images of liquid paraffin droplets on models **B** and **E**. Only on model **B** a bright area was observed around the droplet, which corresponds to water flowing under capillary action into the groove network on the rough surface. The wicking velocity was, therefore,

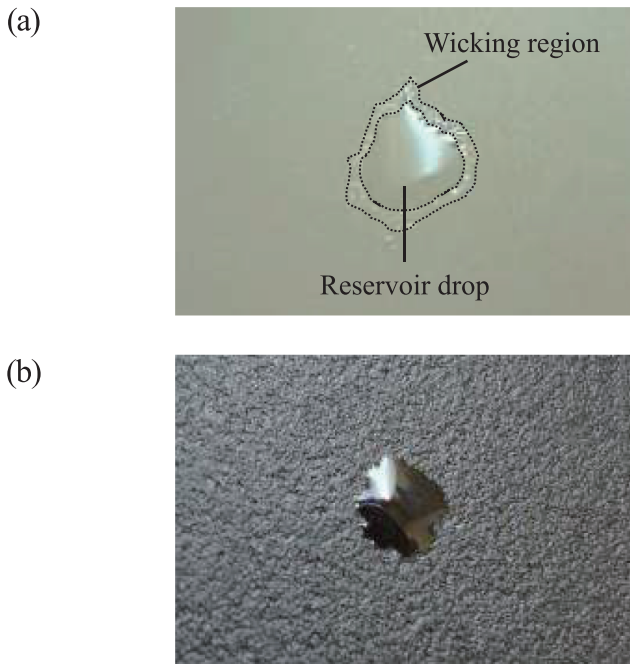


Fig. 4 Images of liquid paraffin droplets on artificial skin models **B**(a) and **E**(b).

greater than that of the spreading velocity. Dussaud *et al.* studied liquid transport in the networked microchannels of the surface of skin and detected wicking flows from an initially placed reservoir drop¹²⁾. Adapting the theory for fracture networks to incorporate the treatment of capillary flow in a single V groove with a cuneate cross-section, they described a model to account for the observed flows as a function of the surface tension and viscosity of the liquid, and the shape, depth, and density of the grooves. According to Dussaud *et al.*, the effective grooves per unit surface area of skin is given by

$$K_G = \frac{l_T \kappa_s}{2} \quad (3)$$

where l_T is the groove length per unit area and κ_s is the permeability of the groove¹²⁾. The liquid velocity at any given distance r depends on the pressure gradient according to

$$v(r) = \frac{K_G}{\mu} \frac{\partial p}{\partial r} \quad (4)$$

where μ is the viscosity of the liquid and p is the pressure gradient¹²⁾. This model is qualitatively consistent with the experimental results of the present study: strong capillary forces due to the high wrinkle density and surface roughness of model **B** induced a low oil contact angle and the formation of a wicking front.

Figure 5(a) shows the friction coefficients when the skin-care cream was applied to the artificial skin models with a contact probe. The dynamic friction coefficient of model **B** was 1.22 ± 0.13 during the 1st slide and decreased to 0.51 ± 0.08 during the 12th slide. The friction coefficients

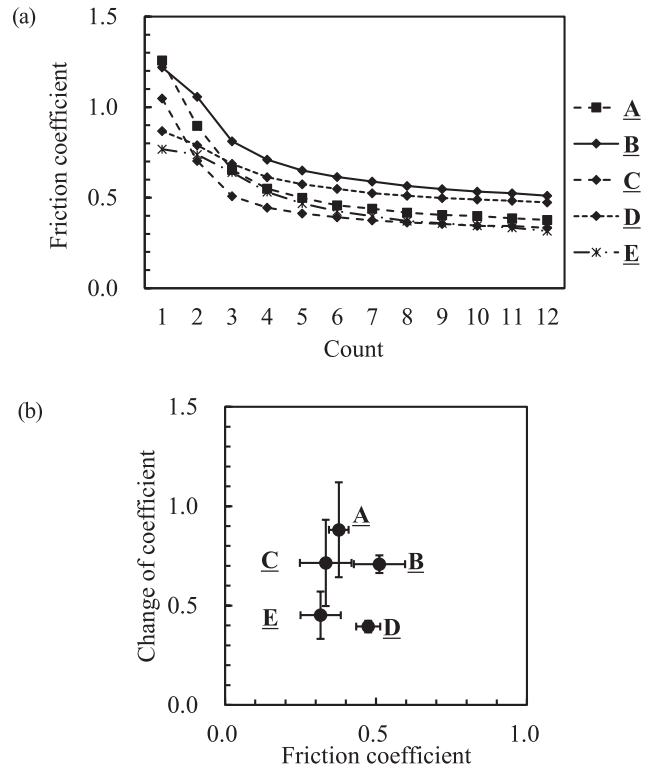


Fig. 5 Friction analyses of artificial skins: (a) change in friction coefficient during reciprocating motion and (b) relationship between the friction coefficient during the 12th cycle and the change in the friction coefficient from the 1st cycle to the 12th cycle.

of all models decreased with the number of slides, but a significant difference was observed in the change of the coefficient. Figure 5(b) shows the dynamic friction coefficient during the 12th slide for each model, as well as the difference between the friction coefficients of the 1st and 12th slides. The friction coefficient for the 12th slide was approximately 0.4, and significant differences were not observed for all models. However, the change in friction coefficient was different for each model. Large changes were observed for models **A**, **B**, and **C**: 0.88 ± 0.24 , 0.71 ± 0.04 , and 0.71 ± 0.22 , respectively. We speculate that the change in friction coefficient is related to the surface roughness; models **A**, **B**, and **C** with large R_a have lower frictional resistance due to the permeation of the cream into the surface grooves.

4 DISCUSSION

Of the five skin models prepared in this study, only model **B** belongs to a similar group as human skin because the following three characteristics are present. The first and second characteristics are smooth and moist feels, which were correlated with the contact angle of oil. When

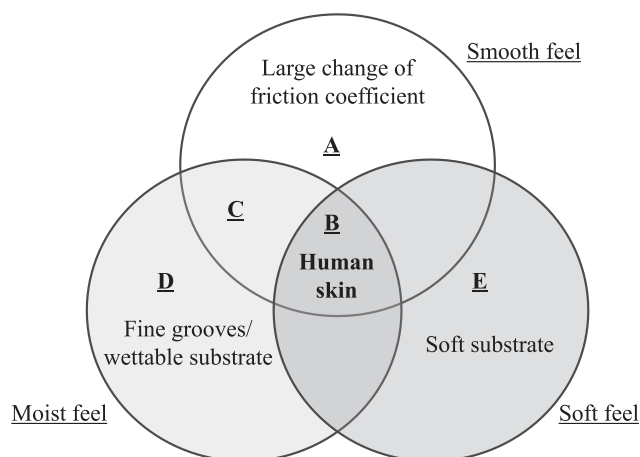


Fig. 6 Necessary conditions for human skin-like texture.

the contact angle of oil on the model skin is smaller, that is, when the wettability toward oil is larger, the scores of these feels increase. This indicates that smoothness and moistness are enhanced by oil spreading over the surface and forming a thin film. The third characteristic is soft feel, which was correlated with the Young's modulus of the skin model material. If the Young's modulus is larger, the soft feel score decreases. This indicates that the soft feel is enhanced by using a substrate with a low elastic modulus.

We propose that these three characteristics are necessary for a realistic artificial skin model (Fig. 6). If one of these characteristics is not present, the group to which the model skin belongs is different from that of human skin in the cluster analysis. In the case of model **A**, the scores for wettability toward oil and softness are too low because the surface grooves and elasticity of the substrate are too large. In the case of model **C**, the soft feel score is too low because the substrate is too hard. In the case of model **E**, the change in friction coefficient and wettability score are too low because the surface grooves are too large.

5 CONCLUSION

In this study, a soft urethane gel was covered with a polyurethane film possessing a microscopically rough surface to prepare an artificial skin model. Sensory evaluation was performed during the application of commercial W/O emulsion cream to the model. Cluster analysis showed that the tactile score of the model was closer to that of human skin than conventional artificial skin. The contact angle 4 minutes after dropping liquid paraffin onto the model was lower than that on a commercial artificial skin product, and the wettability toward oil was also good. In addition, the change in friction of the artificial skin model immediately after cream application was large. The combination of these physical properties is thought to result in the expression of tactile factors similar to those of human

skin. The artificial skin developed herein is expected to be useful for constructing a system to evaluate the feelings experienced when using liquid cosmetics.

Acknowledgment

The present study is supported by The Cosmetology Research Foundation and Grand-in-Aid for Scientific Research on Innovation Areas (No. 16H01661) from MEXT, Japan.

References

- 1) Burke, J.F.; Yannas, I.V.; Quimby, W.C.; Bondoc, C.C.; Jung, W.K. Successful use of a physiologically acceptable artificial skin in the treatment of extensive burn injury. *Ann. Surg.* **194**, 413-448 (1981).
- 2) Tompkins, R.G.; Burke, J.F. Progress in burn treatment and use of artificial skin. *World J. Surg.* **14**, 819-924 (1990).
- 3) MacNeil, S. Progress and opportunities for tissue-engineered skin. *Nature* **445**, 874-880 (2007).
- 4) Shirado, H.; Nonomura, Y.; Maeno, T. Development of artificial skin having skin-like texture (realization and evaluation of human skin-like texture by emulating surface shape pattern and elastic structure). *Trans. Jpn. Soc. Mech. Eng., Ser. C* **73**, 541-546 (2007).
- 5) Derler, S.; Schrade, U.; Gerhardt, L.-C. Tribology of human skin and mechanical skin equivalents in contact with textiles. *Wear* **263**, 1112-1116 (2007).
- 6) Cannata, G.; Maggiali, M.; Metta, G.; Sandini, G. An embedded artificial skin for humanoid robot. *Proc. IEEE Int. Conf. Multisens. Fusion Integr. Intell. Syst.* 434-438 (2008).
- 7) Shao, F.; Childs, T.H.C.; Henson, B. Developing an artificial fingertip with human friction properties. *Tribol. Int.* **42**, 1575-1581 (2009).
- 8) Park, Y.; Chen, B. Design and fabrication of soft artificial skin using embedded microchannel and liquid conductors. *IEEE Sens. J.* **12**, 2711-2718 (2012).
- 9) Nachman, M.; Franklin, S.E. Artificial skin model simulating dry and moist in vivo human skin friction and deformation behavior. *Tribol. Int.* **97**, 431-439 (2016).
- 10) Kuramitsu, K.; Nomura, T.; Nomura, S.; Maeno, T.; Nonomura, Y. Friction evaluation system with a human finger model. *Chem. Lett.* **42**, 284-285 (2013).
- 11) Yamaguchi, A.; Kikegawa, K.; Imai, Y.; Nonomura, Y. Friction phenomena in the application process of cosmetic foundation. *J. Jpn. Soc. Colour Mater.* **89**, 294-298 (2016).
- 12) Dussaud, A.D.; Adler, P.M.; Lips, A. Liquid transport in the networked microchannels of the skin surface.

- Langmuir* **19**, 7341-7345 (2003).
- 13) Brandrup, J.; Immergut, E. H. *Polymer Handbook*, 3rd edn., Wiley Intersciences, New York (1990).
 - 14) Ginn, M.E.; Noyes, M.E.; Jungermann, E. The contact angle of water on viable human skin. *J. Colloid Interface Sci.* **26**, 146-151 (1968).
 - 15) Ohzono, T.; Monobe, H. Microwrinkles: Shape-tunability and applications. *J. Colloid Interface Sci.* **368**, 1-8 (2012).
 - 16) Cerda, E.; Mahadevan, L. Geometry and physics of wrinkling. *Phys. Rev. Lett.* **90**, No. 074302 (2003).
 - 17) Wenzel, R.N. Resistance of solid surfaces to wetting by water. *Ind. Eng. Chem.* **28**, 988-994 (1936).
 - 18) Baret, J.; Decre, M. Transport dynamics in open microfluidic grooves. *Langmuir* **23**, 5200-5204 (2007).
-